Naval Research Laboratory
Stennis Space Center, MS 39529-5004

NRL/MR/7320--13-9443

Comparison of 1-D and 3-D Simulations of Upper-Ocean Structure Observed at the Hawaii Ocean Time Series Mooring

Paul J. Martin
Patrick J. Hogan
James G. Richman

Ocean Dynamics and Prediction Branch
Oceanography Division

January 23, 2013

REPORT DOCUMENTATION PAGE

Form Approved
OMB No. 0704-0188

1. REPORT DATE *(DD-MM-YYYY)*: 23-01-2013

2. REPORT TYPE: Memorandum Report

3. DATES COVERED *(From - To)*:

4. TITLE AND SUBTITLE

Comparison of 1-D and 3-D Simulations of Upper-Ocean Structure Observed at the Hawaii Ocean Time Series Mooring

5a. CONTRACT NUMBER

5b. GRANT NUMBER

5c. PROGRAM ELEMENT NUMBER
0602435N

6. AUTHOR(S)

Paul J. Martin, Patrick J. Hogan, and James G. Richman

5d. PROJECT NUMBER

5e. TASK NUMBER

5f. WORK UNIT NUMBER
73-6288-02-5

7. PERFORMING ORGANIZATION NAME(S) AND ADDRESS(ES)

Naval Research Laboratory
Oceanography Division
Stennis Space Center, MS 39529-5004

8. PERFORMING ORGANIZATION REPORT NUMBER

NRL/MR/7320--13-9443

9. SPONSORING / MONITORING AGENCY NAME(S) AND ADDRESS(ES)

Office of Naval Research
One Liberty Center
875 North Randolph Street, Suite 1425
Arlington, VA 22203-1995

10. SPONSOR / MONITOR'S ACRONYM(S)

ONR

11. SPONSOR / MONITOR'S REPORT NUMBER(S)

12. DISTRIBUTION / AVAILABILITY STATEMENT

Approved for public release; distribution is unlimited.

13. SUPPLEMENTARY NOTES

14. ABSTRACT

Local, one-dimensional (1-D) simulations of the upper-ocean structure observed at the Hawaii Ocean Time Series (HOTS) mooring located 100 km north of Oahu are compared with output from the operational Global NCOM ocean forecast system at the location of the mooring. The observations from the mooring indicate that the upper-ocean density structure and mixed-layer depth (MLD) in this area are significantly affected by the extensive eddy field that exists there. Local, 1-D simulations do not account for the modulation of the upper-ocean density structure by the eddies. However, Global NCOM, along with the data assimilation that it uses, provides a reasonably accurate simulation of the eddies and does a fairly good job of accounting for the effect of the eddies on the upper-ocean density structure and MLD. Comparison of atmospheric fields from NOGAPS, which are used by Global NCOM, with observations from the mooring show fairly good agreement, which contributes to the skill shown by Global NCOM in simulating the sea-surface temperature and MLD observed at the mooring.

15. SUBJECT TERMS

WHOTS mooring, Surface mixed layer, Air-sea fluxes, Ocean mixing, Ocean modeling

16. SECURITY CLASSIFICATION OF: a. REPORT	b. ABSTRACT	c. THIS PAGE	17. LIMITATION OF ABSTRACT	18. NUMBER OF PAGES	19a. NAME OF RESPONSIBLE PERSON
Unclassified Unlimited	Unclassified Unlimited	Unclassified Unlimited	Unclassified Unlimited	21	Paul Martin
					19b. TELEPHONE NUMBER *(include area code)* (228) 688-5447

Standard Form 298 (Rev. 8-98)
Prescribed by ANSI Std. Z39.18

CONTENTS

COMPARISON OF 1-D AND 3-D SIMULATIONS OF UPPER-OCEAN STRUCTURE OBSERVED AT THE HAWAII OCEAN TIME SERIES MOORING

1. INTRODUCTION

Woods Hole Oceanographic Institution (WHOI) has maintained a data mooring about 100 km north of Oahu at about 158 °W, 22.75 °N from August 2004 to the present. This is referred to as the WHOI Hawaii Ocean Time Series (WHOTS) Mooring. The mooring records both surface meteorological observations and subsurface ocean observations down to a depth of about 155 m.

Pal et al. (2012) used data from the mooring to perform local, one-dimensional (1-D) surface mixed layer (ML) simulations with several turbulence models for the period 18 March 2005 to 15 June 2006. These local ML simulations were able to do a reasonably good job of hindcasting the changes in the upper ocean observed by the mooring. However, these simulations were not able to account for the significant modulation of the upper-ocean density structure and ML depth (MLD) by the extensive eddy field that exists in this area.

This report compares local, 1-D simulations of the upper ocean at the location of the WHOTS mooring with output from the Global NCOM (G-NCOM) model (Barron et al. 2004), which was running operationally at the Naval Oceanographic Office at the time the observations were taken. G-NCOM uses assimilation of three-dimensional (3-D) temperature and salinity fields derived from satellite altimetry and satellite sea-surface temperature (SST) data to maintain a portrait of the upper-ocean structure that includes the larger-scale fronts and eddies that are resolved by the satellite data. Hence, G-NCOM should be able to account for some of the effects of the large-scale eddies on the upper-ocean density structure in the area of the WHOTS mooring.

2. DESCRIPTION OF THE WHOTS MOORING

As noted in the introduction, the WHOTS mooring is located about 100 km north of the island of Oahu at about 158 °W, 22.75 °N, and has been maintained by the WHOI from August 2004 to the present. The mooring consists of a 2.7-m Surlyn buoy that is tethered to the sea floor at a depth of about 4700 m. Data acquired by the mooring consist of both surface meteorological and subsurface ocean observations. The meteorological and ocean data can be downloaded from the WHOTS web site at *www.soest.hawaii.edu/whots/*.

The time period of the 1-D simulations conducted at the mooring site by Pal et al. (2012) is from 18 March 2005 to 15 June 2006, and this is the time period that is investigated here. This time period is included within the first two deployments of the WHOTS mooring, which were from 13 August 2004 to 25 July 2005 and from 28 July 2005 to 24 June 2006, respectively.

Manuscript approved October 10, 2012.

The meteorological observations at the mooring are measured by two complete Air-Sea Interaction Meteorological (ASIMET) systems, and include air temperature and relative humidity (at 3.08-m height), SST (at 1-m depth), barometric pressure (at 3.225-m height), wind speed and direction (at 3.47-m height), incoming shortwave and longwave radiation (at 3.58-m height), and precipitation (at 3.21-m height). The meteorological measurements are recorded every minute and hourly averages are transmitted via the Argos satellite system.

Subsurface measurements at the mooring include two Vector-Measuring Current Meters (VMCMs) at 10 and 30 m, an RDI Acoustic Doppler Current Profiler (ADCP) at 125 m, and SEACAT and MicroCat temperature and salinity observations at depths of 1, 15, 25, 35, 40, 45, 50, 55, 65, 75, 85, 95, 105, 120, 135, and 155 m. These SEACAT and MicroCat temperature and salinity observations are used to define the upper-ocean density structure at the mooring. The observations at 45, 85, 105, 120, and 155 m depth also include pressure.

3. DESCRIPTION OF GLOBAL NCOM

G-NCOM is a global ocean model that was developed at the Naval Research Laboratory at Stennis Space Center, MS (Barron et al. 2004). G-NCOM is run operationally at the Naval Oceanographic Office, which is also located at Stennis Space Center, MS. However, G-NCOM is currently in the process of being replaced by a global version of the Hybrid-Coordinate (HYCOM) Ocean Model.

G-NCOM is run on a tri-polar, curvilinear, horizontal grid. This grid uses spherical geometry at latitudes below about 32 °N, but deviates from spherical above this latitude to avoid convergence of the meridional coordinates at the north pole in the Arctic Ocean, i.e., instead of having a singularity at the north pole, which is over water, the grid has singularities over land in northern Canada and northern Russia. Communication across the "seam" in the grid that crosses the Arctic Ocean and across the east-west seam, which is located at about 80 °E, is handled by the MPI communication that is used for the domain decomposition procedure used for computing on multiple processors.

The horizontal dimensions of the G-NCOM grid are 2048 by 1280. The horizontal grid spacing ranges from a maximum of about 19.6 km at the equator down to roughly 8-12 km in the Arctic Ocean and down to about 4 by 11 km in the east-west and north-south directions, respectively, near Antarctica. The vertical grid consists of 40 layers, with an upper-layer thickness of 1 m in deep water and a uniform (logarithmic) stretching to the bottom at 5500 m. The upper 19 layers of the grid from the surface to 138-m depth use sigma coordinates and these compress in water shallower than 138 m in the manner of a typical sigma-coordinate grid. The deeper layers remain at a fixed depth. Hence, in water shallower than 138 m the grid is sigma coordinate and in water deeper than 138 m the vertical layers are approximately level.

The air-sea fluxes used to drive G-NCOM are obtained from the 0.5° NOGAPS model that is run at FNMOC in Monterey, CA (Rosmond et al. 2002). The surface wind stress and solar and longwave radiation are taken directly from NOGAPS. The latent and sensible heat fluxes are computed using the SST predicted by NCOM and the wind speed, humidity, and air temperature from NOGAPS, which provides some feedback from the NCOM SST in the calculation of the surface heat fluxes. This also helps avoid unrealistic heating and cooling that can occur in shallow water when there is no feedback from the predicted SST to the surface heat flux to restrain the heat flux.

The G-NCOM SST is relaxed to a satellite SST analysis and the SSS is relaxed to a monthly surface salinity climatology. The relaxation rates are 2 m/d for the SST and 0.5 m/d for the SSS. A time scale for the SST and SSS relaxation can be estimated by dividing the MLD by these relaxation rates, e.g., for a MLD of 20 m, the SST relaxation time scale is about 10 days and that for the SSS is about 40 days.

The data assimilation used in G-NCOM is a relaxation to a 3-D temperature and salinity analysis derived from satellite altimeter and SST data. The relaxation time scale is weaker near the surface and stronger at depth and is given by $t_s/(1-\exp[z/d_s])$, where the time scale t_s is 48 h, the depth scale d_s is 200 m, and z is the depth in meters (positive upwards).

4. SIMULATION WITH A LOCAL 1-D MODEL

A local, 1-D simulation of the changes in the upper ocean at the location of the WHOTS mooring was conducted with NCOM. NCOM was run in what we refer to as pseudo 1-D mode using a horizontal grid of 2 by 2 points and doubly-periodic lateral boundary conditions. The vertical grid consisted of 40 layers with an upper-layer thickness of 1 m and a uniform stretching to a maximum depth of 5500 m. This is the same as the vertical resolution used by G-NCOM in deep water and is typical of the vertical resolution used in regional NCOM simulations.

Air-sea fluxes for the local, 1-D simulation were computed from the WHOTS mooring data using fairly standard air-sea flux formulas. The surface wind stress was computed using the neutral drag coefficient of Garratt (1977), the stability correction of Kondo (1975), and the boundary layer correction to 10-m height from Liu et al. (1979). A 6% albedo was used to account for the reflected solar radiation. Cloud cover was estimated from the shortwave radiation measurements and this cloud cover was used to estimate the net longwave radiation using the formula of Berliand (Wyrtki, 1965).

The latent and sensible heat fluxes were computed during the simulation using the model-predicted SST and the wind speed, air-temperature, and humidity from the mooring. The surface moisture flux was taken to be zero. The penetration of solar radiation below the ocean's surface was parameterized using the Jerlov (1968) extinction profile for Type IA seawater, which is for fairly clear ocean water.

The background vertical mixing rate for momentum, heat, and salt was taken to be 0.1 cm^2/s. The ML model used was the Mellor-Yamada Level 2 turbulence model (Mellor and Yamada 1974; Martin 2000), with the Large et al. (1994) enhancement to account for intermittent mixing near the base of the ML by internal waves. Note that this is also the vertical mixing scheme used by G-NCOM. A linear damping term in the momentum equations with a damping time scale of 10 d was used to provide some damping of inertial oscillations, since the normal horizontal and vertical dispersion of these motions cannot be accounted for in a 1-D simulation such as is being conducted here. The model was run with a timestep of 300 s. Initial temperature and salinity profiles for 18 May 2005 were obtained from the WHOTS mooring data.

Figure 1 shows a comparison of the observed (black) and simulated (red) SST, MLD, and isotherm depths (ISODs) for this simulation. The SST and MLD errors for the simulation with respect to the mooring observations are provided in Table 1. Following Pal et al. (2012), the MLD in Fig. 1 and Table 1 is computed as the depth where the density is 0.092 kg/m^3 greater than that at the surface, or at the shallowest available value. For the range of SST at the mooring, this density change is equivalent to a temperature decrease of about 0.3 °C at constant salinity.

Table 1 — SST and MLD Errors for Simulations at WHOTS Mooring

model	atm forcing	SST (°C)			MLD (m)		
		mean	rms	correlation	mean	rms	correlation
Local NCOM	WHOTS	-0.15	0.29	0.98	-4.1	25.3	0.68
Global NCOM	NOGAPS	-0.13	0.37	0.96	-1.7	22.7	0.72
Local NCOM	NOGAPS	-0.36	0.49	0.96	-4.3	28.8	0.60

Results are similar to those reported by Pal et al. (2012) for their local, 1-D, simulations. The simulated MLD shows periods of time when it is shallower than the observed MLD and periods when it is deeper. As noted by Pal et al. (2012), this is, in part, due to the modulation of the upper-ocean thermal structure by the propagation of eddies past the mooring location. The observed ISODs in Fig. 1 show large excursions of the 22 °C isotherm caused by the propagation of the eddies past the mooring. The period of these isotherm excursions is on the order of 60-80 days. The deep isotherms for the local, 1-D simulation in Fig. 1 are flat since such advective processes are not accounted for.

The envelope of the simulated SST in Fig. 1 follows the observed SST very well, with a mean difference of -0.15 °C and a root-mean-square (rms) difference of 0.29 °C (Table 1). Note that the calculation of the latent and sensible heat fluxes using the model-simulated SST provides some feedback from the model SST to the surface heat flux and helps keep the simulated SST tracking the observed SST. The spikes in the simulated SST, which occur during periods of light winds when the MLD becomes very shallow, are, on average, fairly consistent with the magnitude of the observed SST spikes.

5. RESULTS FROM GLOBAL NCOM AT WHOTS MOORING

Figure 2 shows a snapshot of the temperature at 150-m depth from the G-NCOM output for 18 March 2005, the beginning of the time period being investigated. The location of the WHOTS mooring is shown by the red dot north of Oahu. The G-NCOM temperature at 150 m shows the eddy field that occurs in this area. The eddies at this latitude have a mean spacing of about 450 km and propagate westward at a speed of about 6 km/d, which gives a mean period of about 75 d; however, there is a lot of variability in these values. The eddies are sufficiently large to be well resolved by the satellite observations and, hence, are present in the 3-D temperature and salinity analyses to which the temperature and salinity fields in G-NCOM are relaxed. Hence, the location, size, and strength of the large-scale eddies in G-NCOM should be approximately correct.

Figure 3 shows a comparison of SST, MLD, and ISODs from G-NCOM interpolated to the location of the WHOTS mooring (red) with observations from the mooring (black). Errors for the G-NCOM SST and MLD relative to the mooring observations are listed in Table 1. The MLD predicted by G-NCOM is an improvement over that predicted by the local, 1-D NCOM simulation in Fig. 1. The predicted MLD is more consistent with the observed MLD in terms of the envelope of shallowing and deepening, and the MLD errors are reduced (Table 1).

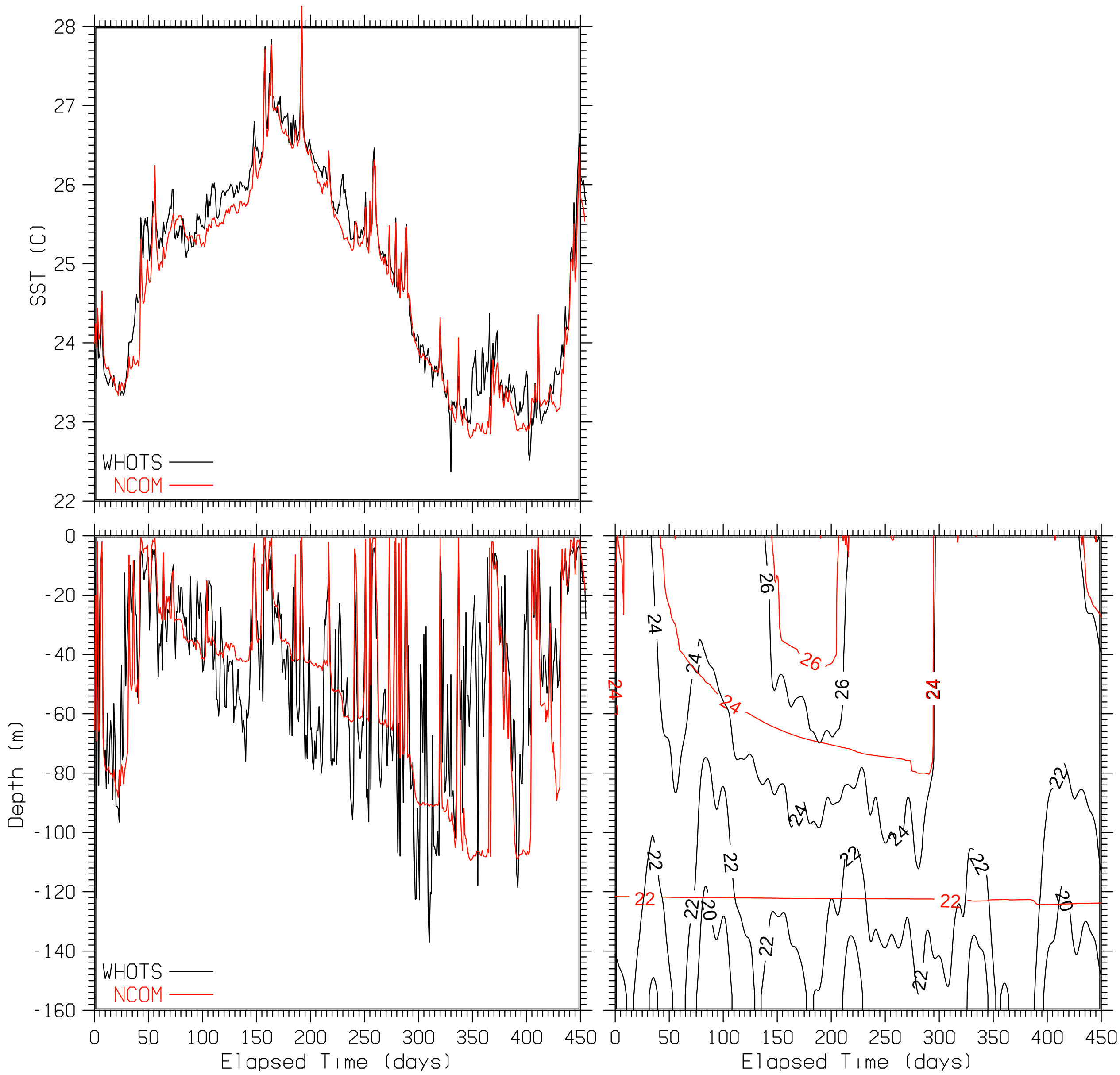

Fig. 1 — SST, MLD, and ISODs at WHOTS mooring for local, 1-D NCOM simulation (red) compared with observed values from the mooring (black)

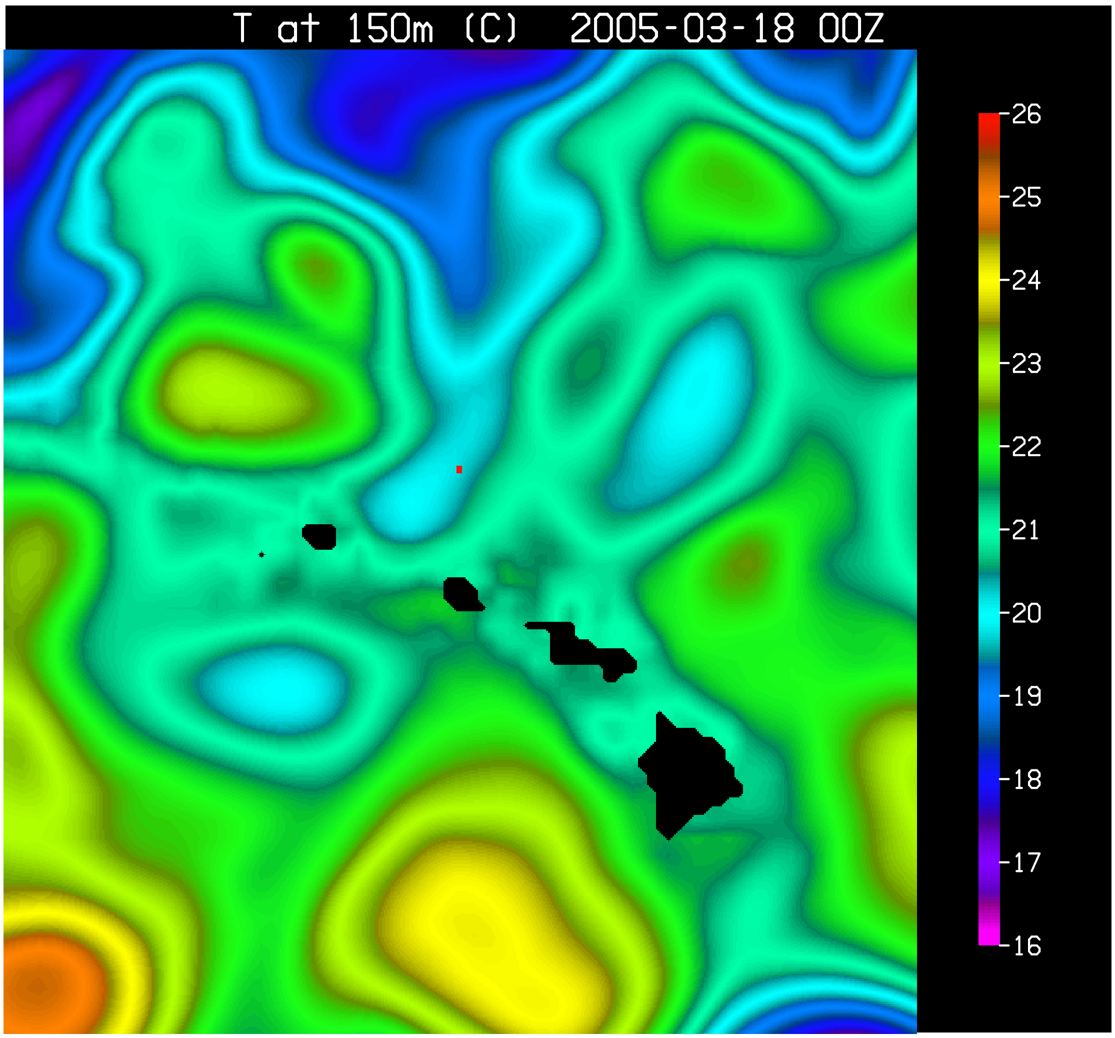

Fig. 2 — Temperature at 150 m from G-NCOM for 18 March 2005; the region shown is 197 to 207 °E, 17 to 27 °N; the location of the WHOTS mooring is shown by the red dot.

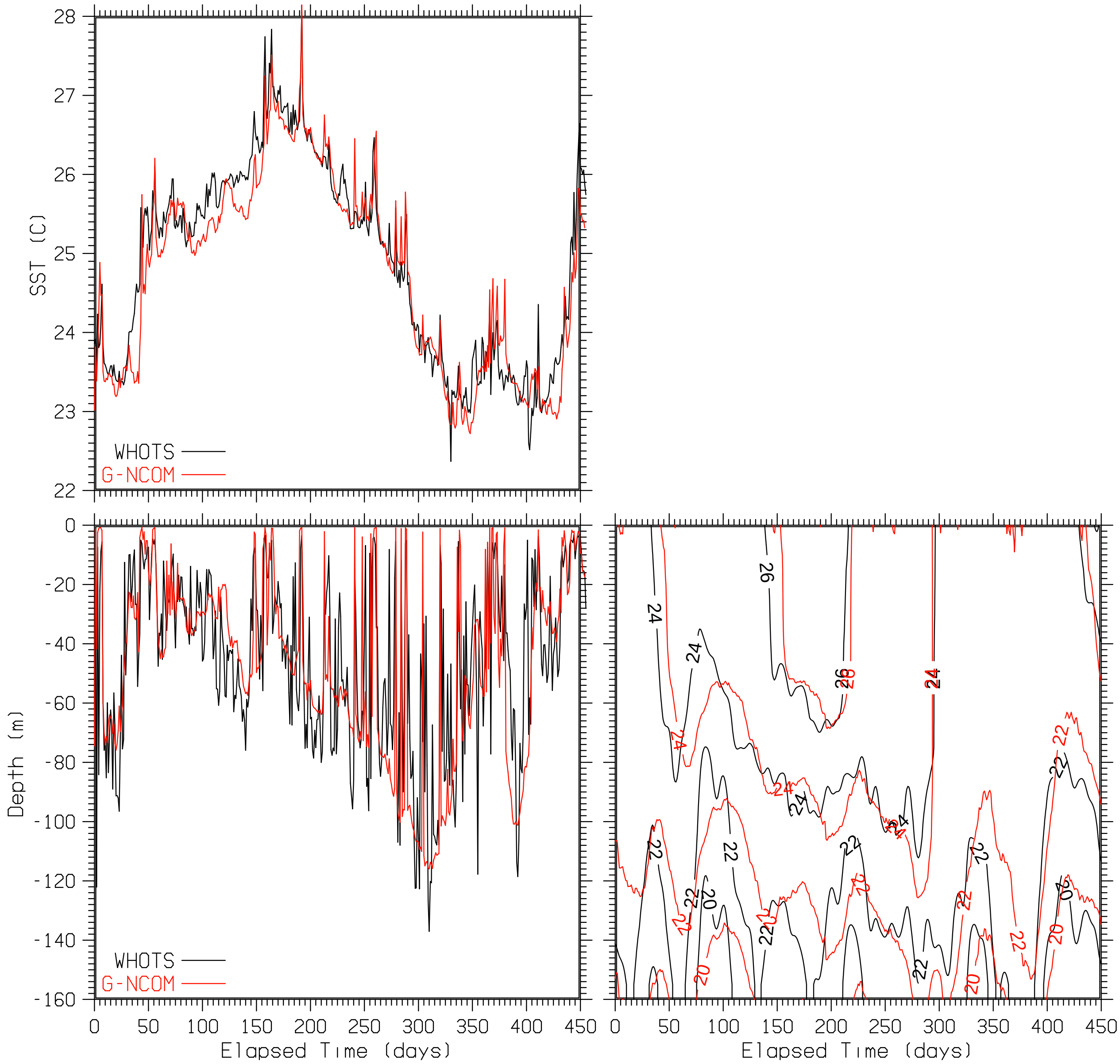

Fig. 3 — SST, MLD, and ISODs at WHOTS mooring from G-NCOM (red) compared with observed values from mooring (black)

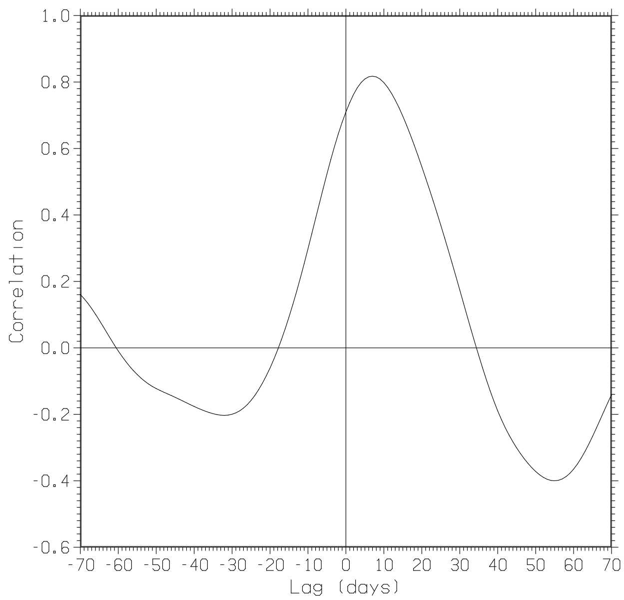

Fig. 4 — Cross correlation between the G-NCOM and WHOTS temperature at 150-m depth.

The ISODs from G-NCOM in Fig. 3 reflect the propagation of eddies past the mooring location. The vertical movement of the 22 °C isotherm is generally consistent with that of the observed 22 °C isotherm in terms of the times of the occurrence of warming and cooling occurring below the ML as the eddies propagate past the mooring.

There is a fairly consistent time lag of a few days apparent in Fig. 3 for the vertical motions of the G-NCOM 22 °C isotherm relative to the observed 22 °C isotherm. A cross-correlation between the G-NCOM and WHOTS mooring temperature at 150-m depth (Fig. 4) indicates a time lag of about 7 days. Cross-correlations of temperature at other depths between 100 and 155 m also show a time lag of about 7 days. This time lag may be partly due to the nudging form of data assimilation that is used in G-NCOM. The relaxation time scale used by G-NCOM is about 4 days at 150 m and about 5 days at 100 m. For a signal with a time period of 75 days, which is roughly the period of the eddies propagating past the mooring, a relaxation time scale of 4–5 days should result in a time lag of 4–5 days. Hence, the time lag of 7 days observed at the WHOTS mooring is slightly greater than what might be expected based on the relaxation time scale used in G-NCOM.

As noted previously, the MLD is computed using a density criteria of 0.092 kg/m^3, which is the density increase that would result from a temperature decrease of 0.3 °C for a fixed salinity. Figure 5 shows the rms error for MLDs computed based on density increases of 0.030 kg/m^3 to 0.306 kg/m^3, which correspond to temperature decreases of 0.1 to 1.0 °C, respectively. Figure 5 shows that the G-NCOM rms MLD error is lower than that for the local, 1-D NCOM simulation for all but the smallest density criteria, and that the G-NCOM MLD error varies within a range of about 2 m as the density criteria used to compute the MLD is increased, whereas the rms MLD error for the local NCOM simulation shows a significant increase. The smaller rms MLD error for local NCOM for the smallest density criteria is likely due to the fact that the local NCOM simulation uses atmospheric forcing derived from the mooring observations, which is more accurate than the NOGAPS atmospheric forcing used by G-NCOM; hence, this simulation might be expected to predict small changes in the near surface stratification better than G-NCOM. However, for larger density criteria, the computed MLD becomes more sensitive to the location of the deeper isopycnals,

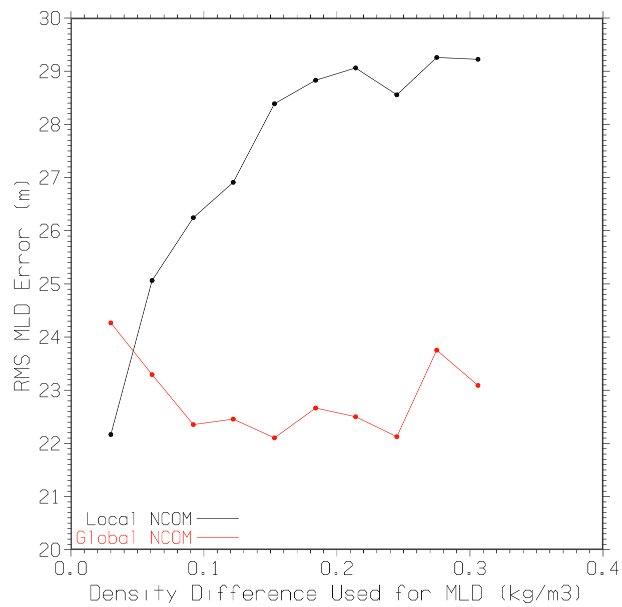

Fig. 5 — RMS MLD error for local, 1-D NCOM simulation (black) and for Global NCOM (red) for different values of the density difference criteria used to calculate the MLD.

which are much better predicted by G-NCOM.

Figure 6 shows a comparison of plots of MLD for the local, 1-D NCOM and G-NCOM simulations computed using density criteria of 0.153 and 0.306 kg/m^3, which correspond to temperature decreases of 0.5 and 1.0 °C, respectively. This figure shows the improvement of G-NCOM over the local NCOM simulation for the prediction of MLD computed for a large density difference criteria. We also tried computing the SST, MLD, and ISODs for the model simulations by first interpolating the model output to the mooring depths, since this might be considered to provide a more appropriate comparison with the subsurface mooring data. However, this did not significantly change the model results or the computed errors.

The SST from G-NCOM in Fig. 3 is not as good as that for the local, 1-D simulation in Fig. 1, but it seems surprisingly good for a SST that is coming from an operational global model. As noted previously, G-NCOM computes its latent and sensible heat fluxes using its predicted SST, similar to what was done with the local, 1-D simulation discussed in the previous section. This provides some feedback from the model's SST to the surface heat flux. G-NCOM also employs a relaxation of its SST to a daily SST analysis with a rate of 2 m/d. However, it is not known whether the observed SSTs from the WHOTS mooring were incorporated into the SST analysis used by G-NCOM.

G-NCOM is driven by air-sea fluxes from the global NOGAPS atmospheric model. Hence, how well the predicted SST spikes, which occur during periods of light winds, agree with the observed SST spikes depends mainly upon how well NOGAPS predicts such light-wind events. A comparison of the G-NCOM and WHOTS SST and MLD in Fig. 3 indicates that many of the light-wind events are predicted fairly well, though sometimes they are under- or over-predicted.

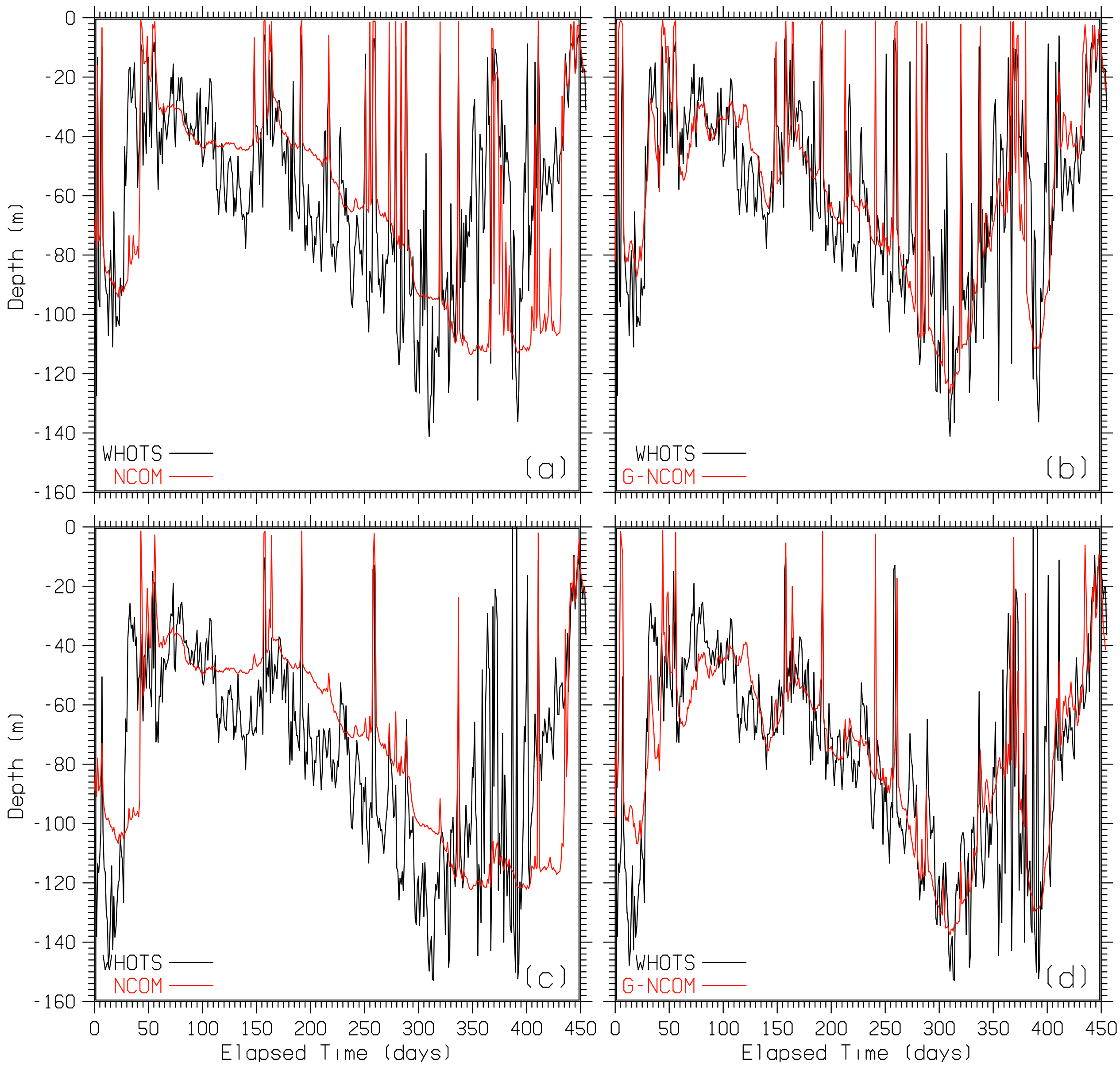

Fig. 6 — Comparison of MLD computed for density difference criteria of 0.153 kg/m^3 (upper two plots) and 0.306 kg/m^3 (lower two plots) for local, 1-D NCOM simulation (plots on left) and for G-NCOM (plots on right). The simulated MLD is shown in red and the observed MLD is shown in black for reference.

6. COMPARISON OF NOGAPS AND WHOTS AIR-SEA FLUXES

The marine data measured at the WHOTS mooring provide an opportunity to compare values of atmospheric fields from NOGAPS with those either measured at the buoy or computed from the buoy observations. Figures 7 to 10 compare the WHOTS and NOGAPS hourly values of the surface wind stress, solar and longwave radiation, air temperature, and water vapor mixing ratio for the first 40 days of the simulation period. These plots provide only a short sampling of the 450 days of the simulation, but they are fairly characteristic of the rest of the time period. Errors for the NOGAPS atmospheric fields with respect to the mooring observations for the entire 450-d period of the simulation are listed in Table 2.

Table 2 — Errors for NOGAPS Surface Atmospheric Fields Relative to WHOTS Observations

field	mean	rms	correlation
E-W Wind Stress (Pa)	0.018	0.040	0.87
N-S Wind Stress (Pa)	-0.001	0.028	0.77
Solar Radiation (W/m^2)	-17.7	128.3	0.91
Net Longwave Radiation (W/m^2)	5.5	16.1	0.37
Air Temperature (°C)	0.49	0.91	0.88
Water Vapor Mixing Ratio (g/kg)	-1.46	1.76	0.86

The surface wind stresses in Fig. 7 illustrate the typical eastward direction of the trade winds at this location. Figure 7 indicates that NOGAPS does a fairly good job of capturing the wind events that occur during this time, such as the period of light winds from the start of the simulation up to about day 8 and the two strong wind events between days 8 and 11 and between days 12 and 15. The skill of NOGAPS in representing these type of wind events allows G-NCOM to predict the SST and MLD with some skill.

The comparison of the WHOTS and NOGAPS solar and net longwave radiation in Fig. 8 shows fairly good agreement. The variation of both of these radiative fluxes depends largely on the cloud cover and atmospheric moisture. The NOGAPS solar radiation shows a low bias during much of the first 40 days in Fig. 8. The mean difference between the NOGAPS and observed solar radiation over the entire 450 days is -18 W/m^2 (Table 2).

The NOGAPS net longwave radiation has a fairly low (0.37) correlation with that computed from the mooring data (Table 2). However, the variability of the net longwave radiation is relatively small as indicated by the rms difference of 16 W/m^2 in Table 2, and the bias of 5.5 W/m^2 is relatively small as well.

The air temperature and atmospheric mixing ratio in Fig. 9 and 10 are shown because they (along with the wind speed and the ocean-model-predicted SST) are used in the calculation of the latent and sensible heat fluxes during the model simulation. The NOGAPS values of these fields agree moderately well with the observed values and capture some of the larger variations. However, the NOGAPS air temperature and mixing ratio show more variability than the observed values.

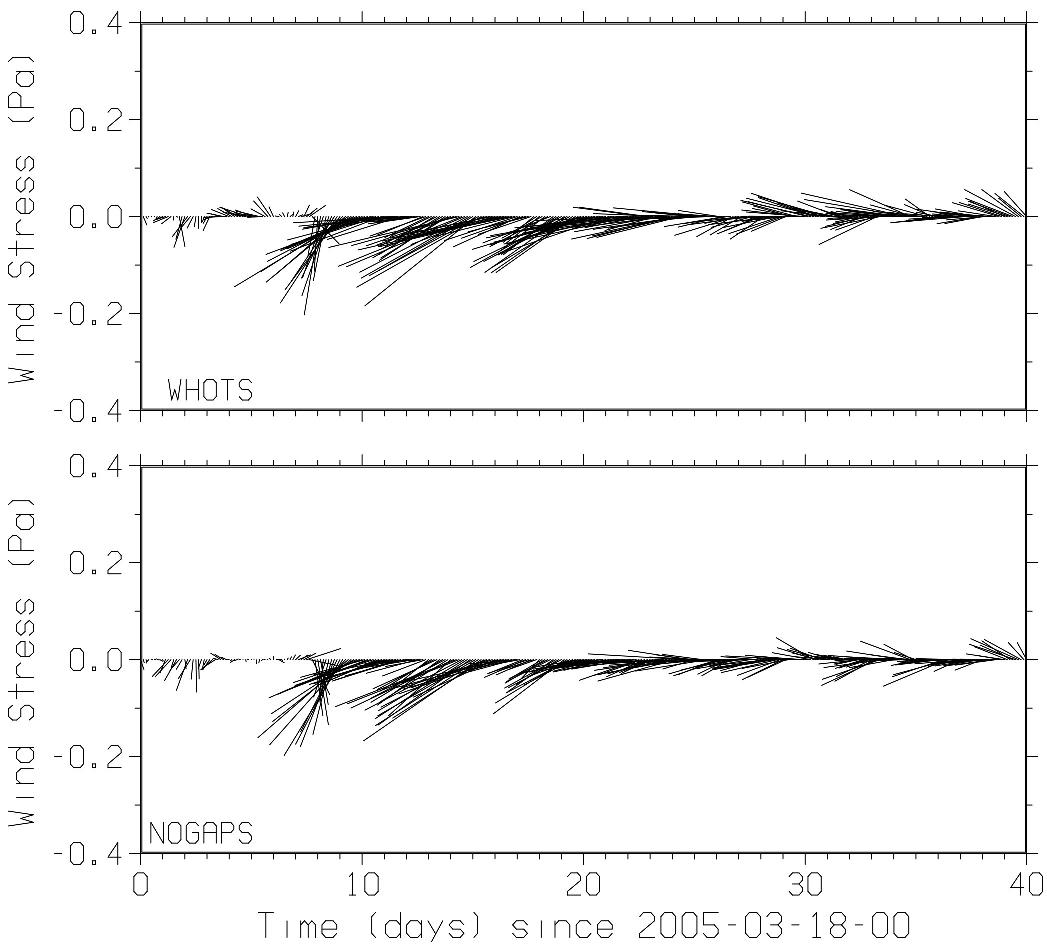

Fig. 7 — WHOTS (upper plot) and NOGAPS (lower plot) surface wind stress for first 40 days of simulation period.

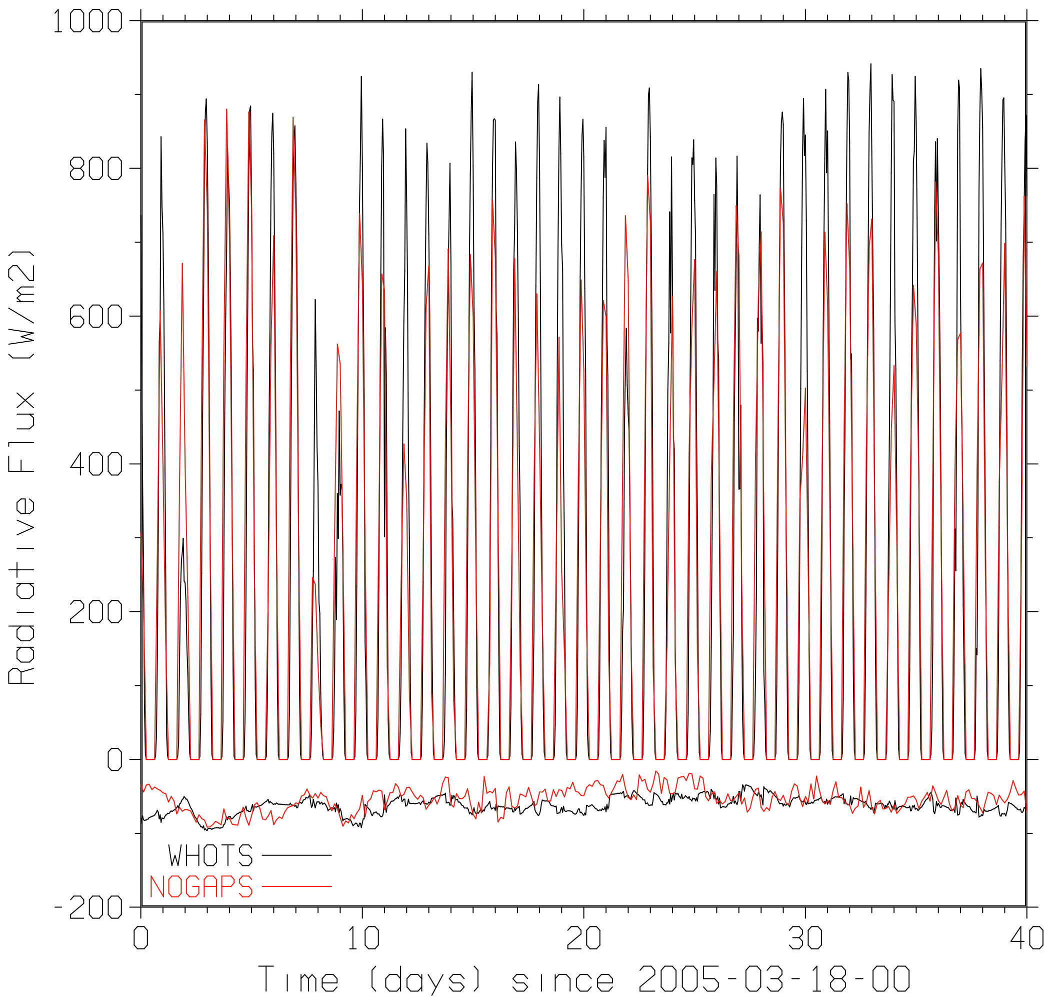

Fig. 8 — WHOTS (black) and NOGAPS (red) solar and net longwave radiation for first 40 days of simulation period.

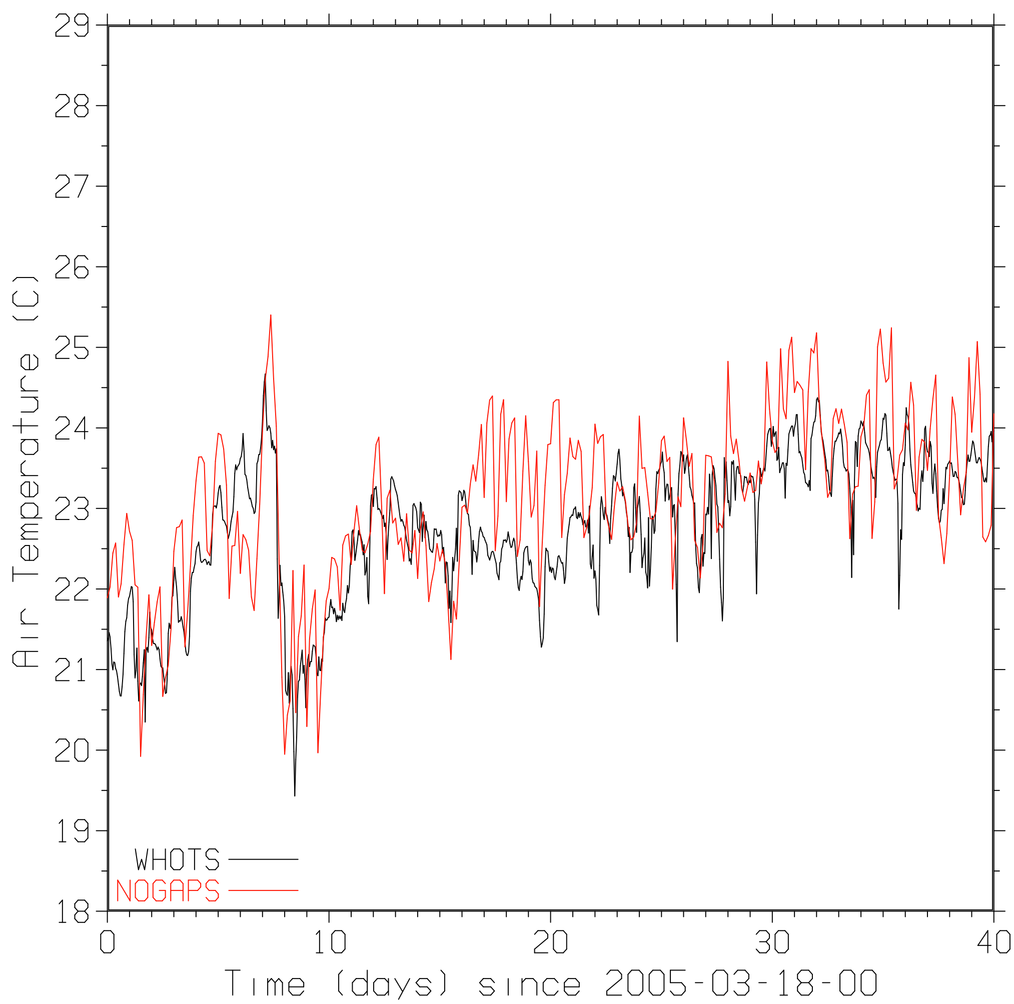

Fig. 9 — WHOTS (black) and NOGAPS (red) surface air temperature for first 40 days of simulation period.

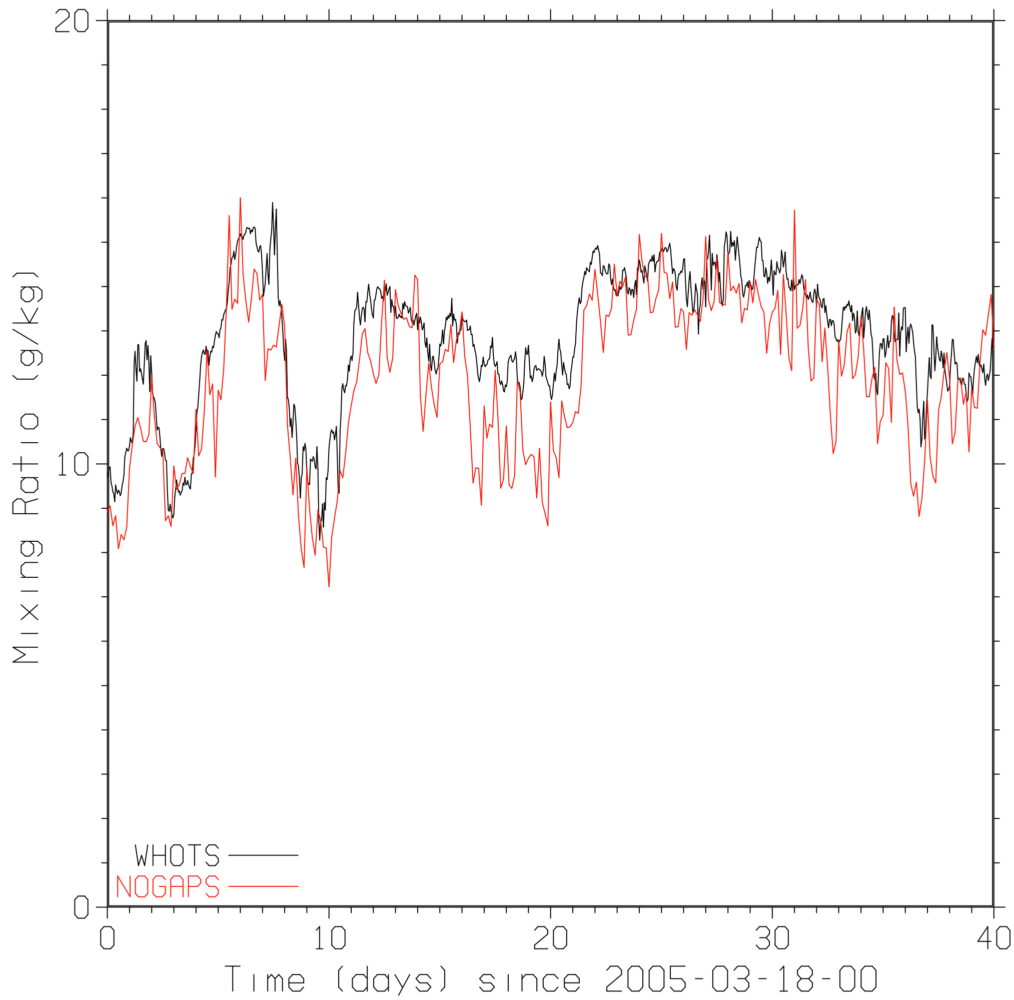

Fig. 10 — WHOTS (black) and NOGAPS (red) surface water vapor mixing ratio for first 40 days of simulation period.

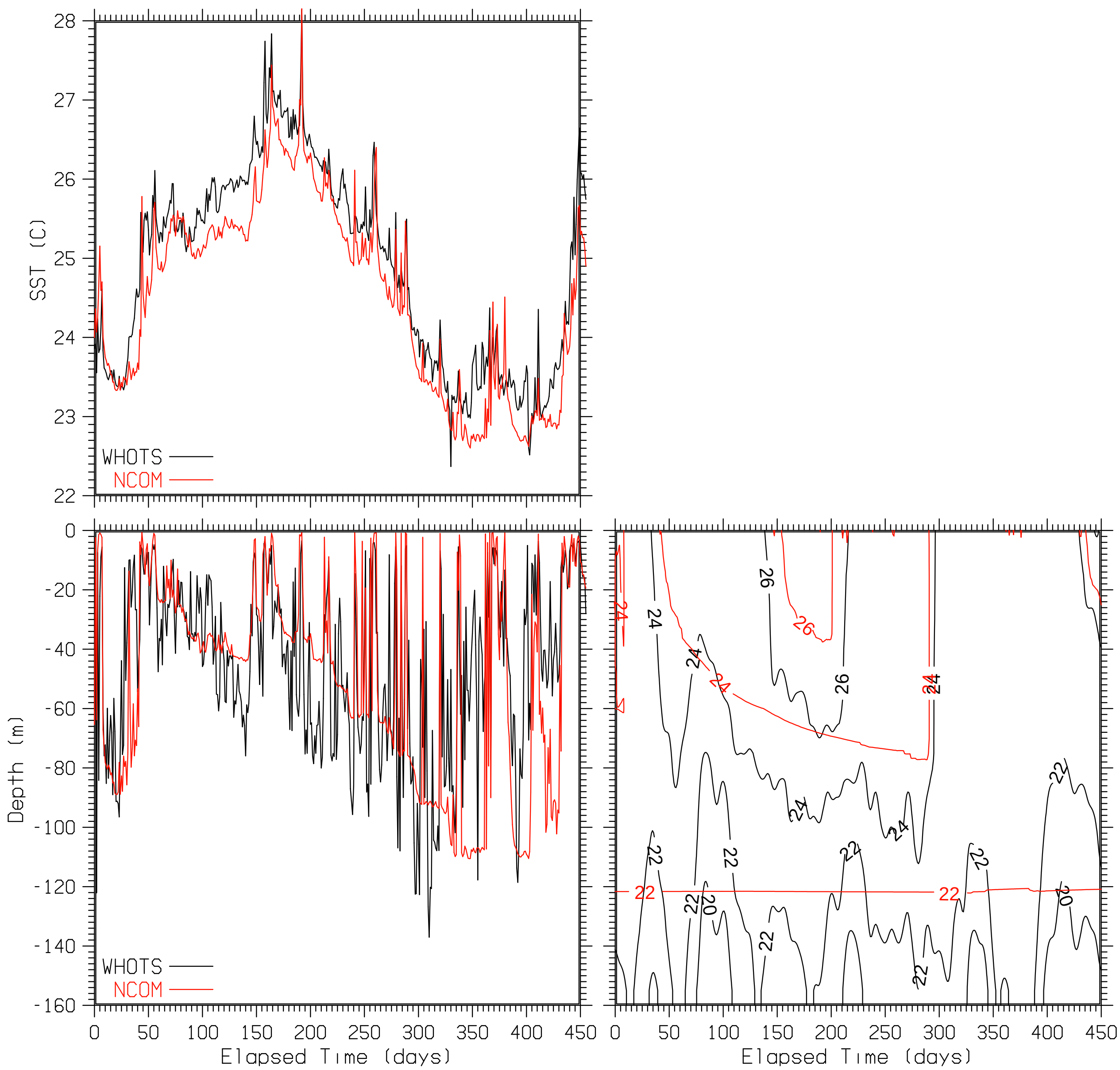

Fig. 11 — SST, MLD, and ISODs at WHOTS mooring for a local, 1-D NCOM simulation that uses NOGAPS atmospheric forcing (red) compared with observed values from the mooring (black)

7. LOCAL 1-D SIMULATION WITH NOGAPS ATMOSPHERIC FORCING

A local, 1-D simulation was conducted at the location of the WHOTS mooring with NCOM with atmospheric forcing from NOGAPS to compare with the earlier, local, NCOM simulation that used atmospheric forcing computed from the mooring observations. Figure 11 shows a comparison of the observed (black) and simulated (red) SST, MLD, and ISODs for this simulation.

Figure 11 can be compared with the previous results shown in Fig. 1 and 3. Note that the MLD in Fig.11 is computed similar to that in Fig. 1 and 3 using a density difference of 0.092 kg/m^3. The SST does not agree with the observed SST as well as the local simulation with atmospheric forcing computed from the mooring observations. This is also indicated by the SST errors in Table 1. This might be expected since the atmospheric forcing computed from the moorings observations should be more accurate than the NOGAPS atmospheric forcing.

The MLD in Fig. 11 is generally similar to that in Fig. 1 and shows the MLD being sometimes shallower than and sometimes deeper than the observed MLD due to the fact that modulation of the upper-ocean thermal structure by the passing eddies is not accounted for. Table 1 indicates that both the SST and MLD errors are higher for this simulation than for the local simulation with atmospheric forcing computed from the mooring data or for the G-NCOM simulation with NOGAPS atmospheric forcing.

8. SUMMARY

Local, 1-D simulations of the upper-ocean structure observed at the WHOTS mooring located 100 km north of Oahu are compared with output from the operational Global NCOM ocean forecast system at the location of the mooring. The observations from the mooring indicate that the upper-ocean density structure and MLD in this area are significantly affected by the extensive eddy field that exists there.

Local, 1-D simulations do not account for the modulation of the upper-ocean density structure by the eddies. However, the data assimilation used by Global NCOM allows it to provide a reasonably accurate simulation of the eddies and an accounting of the effect of the eddies on the upper-ocean density structure and MLD.

Global NCOM shows lower rms MLD errors than the local, 1-D simulation, except for the case where the MLD is computed based on a very small increase in density from that at the surface. The improvement of the rms MLD error for Global NCOM over that of the local, 1-D simulation increases as the density increment used to compute the MLD is increased, which occurs because the MLD computed for larger density increments is more sensitive to the vertical positions of the deeper isopyncals, which are affected by the passing eddies.

Comparison of atmospheric fields from NOGAPS, which are used by Global NCOM, with observations from the mooring show fairly good agreement, which contributes to the skill shown by Global NCOM in simulating the SST and MLD observed at the mooring. However, a local simulation at the WHOTS mooring using NOGAPS atmospheric forcing shows larger errors than the local simulation using atmospheric forcing computed from the mooring observations, which indicates that the mooring observations provide more accurate atmospheric forcing than NOGAPS, as would be expected.

9. ACKNOWLEDGMENTS

This work was funded through the 6.2 NRL Core Project "Full Column Mixing for Numerical Ocean Models," Program Element Number 0602435N.

10. REFERENCES

Barron, C.N., A.B. Kara, H.E. Hurlburt, C. Rowley, and L.F. Smedstad (2004). "Sea Surface Height Predictions From the Global Navy Coastal Ocean Model (NCOM) During 1998–2001," *J. Atmos. Oceanic Technol.* **21**(12), 1876–1894.

Garratt, J. R., (1977). "Review of Drag Coefficients Over Oceans and Continents," *Mon. Weather Rev.* **105**, 915–929.

Jerlov, N. G. (1968). *Optical Oceanography*, (Elsevier Publ. Co., Inc., New York), 194 pp.

Large, W.G., J.C. McWilliams, and S. Doney (1994). "Oceanic Vertical Mixing: a Review and a Model with a Nonlocal Boundary Layer Parameterization," *Rev. Geophys.* **32**, 363–403.

Kondo, J., (1975). "Air-sea Transfer Coefficients in Diabatic Conditions," *Boundary-Layer Meteorology* **9**, 91–112.

Liu, W.T., K.B. Katsaros, and J.A. Businger (1979). "Bulk Parameterization of Air-sea Exchanges of Heat and Vapor Including the Molecular Constraints at the Interface," *J. Atm. Sci.* **36**, 1722–1735.

Martin, P.J. (2000). "A Description of the Navy Coastal Ocean Model Version 1.0," NRL Report NRL/FR/7322–00-9962, Naval Research Laboratory, SSC, MS 39529, 42 pp.

Mellor, G.L. and T. Yamada (1974). "A Hierarchy of Turbulence Closure Models for Planetary Boundary Layers," *J. Atmos. Sci.* **31**, 1791–1806.

Pal, R., J.G. Richman, and A.J. Wallcraft (2012). "Modeling the Surface Mixed Layer: A Case Study at the Hawaii Ocean Time-Series Station," in preparation.

Rosmond, T.E., J. Teixeira, M. Peng, T.F. Hogan, and R. Pauley (2002). "Navy Operational Global Atmospheric Prediction System (NOGAPS): Forcing for Ocean Models," *Oceanography* **15**, 99–108.

Wyrtki, K. (1965). "The Average Annual Heat Balance of the North Pacific Ocean and its Relation to Ocean CircuLation," *J. Geophys. Res.* **70**, 4547–4559.